PHYSICAL REVIEW A **109**, L060802 (2024)

Letter

Chiral photoelectron spectroscopy using unpolarized light

Yoshi-Ichi Suzuki [*]
School of Medical Technology, Health Sciences University of Hokkaido, 1757 Kanazawa, Tobetsucho, Ishikari, Hokkaido 061-0293, Japan

(Received 28 January 2024; revised 2 May 2024; accepted 30 May 2024; published 17 June 2024)

This Letter studies the symmetry properties of general vector correlations resulting from one-photon excitation of chiral molecules. We show that the parity-odd second rank tensor is nonzero for molecules in all chiral point groups C_n, D_n, T, O, and I. This chirality-sensitive tensor is nonzero even for chiral isotopomers excited by linearly polarized or even unpolarized light. We develop an irreducible tensor theory based on Curie's limiting groups. As an example of vector correlations, recoil-frame photoelectron angular distributions (RFPADs) are calculated for methyloxirane and CHF^{35}Cl^{37}Cl. The difference in the RFPAD between a chiral molecule and its mirror image reaches ±35% of the maximum value for the RFPAD for unpolarized light and ±55% of the value for linearly polarized light. Chiral sensitivity in vector correlation is a quite general phenomenon arising from one-photon excitation by unpolarized and linearly polarized light, and we expect it to be of great importance in time-resolved spectroscopy of ultrafast chemical reactions.

DOI: 10.1103/PhysRevA.109.L060802

The photoelectron angular distribution of chiral molecules exhibits forward-backward asymmetry [1–3] that is dependent on the helicity of the light to which these molecules are exposed. Specifically, this asymmetry only appears in the case that circularly polarized light is employed, while the He I and He II light sources [4–6] that are typically employed for photoionization are unpolarized. In addition, short pulses of linearly polarized light have been frequently used to study ultrafast chemical reactions, while the generation of ultrashort pulses of circularly polarized light [7,8] is still under development. At present, several techniques allow chiral molecules to be differentiated using linearly polarized light [9–16] or unpolarized light [17,18]. Cherebkov pointed out that a longitudinal component of electron spin, due to molecular chirality, exists even for unpolarized light [17–19], although this remains to be verified experimentally. This theory points to the importance of symmetry and vector correlation.

As for symmetry, selective elimination and generation of chiral molecules over their mirror images in the gas and liquid phases require external fields lacking any rotoreflection (that is, improper rotation) symmetry, such as circularly polarized light [20], spin-polarized electrons [21], and combination of electromagnetic fields [22,23]. Conversely, chiral molecules can exhibit a lower symmetry response to external fields, such as the forward-backward asymmetry of the photoelectron angular distribution [1–3], an electric dipole moment induced by magnetic fields [24] or orthogonal electric fields [25–27], and some other examples discussed by Marichez *et al.* [28] and by Ordonez and Smirnova [29]. In this way, we may distinguish chiral molecules by the symmetry of their response to unpolarized light, rather than by the difference in response between left- and right-handed circularly polarized light.

Circular dichroism in vector correlations [30–33] may not be related molecular chirality, because vector correlation [11,17,31–41] can express symmetries that are impossible with a simple one-particle angular distribution (AD). As an example, the two-particle AD function $x_1y_2 - x_2y_1$ has the same symmetry as rotational motions [28], such as angular momentum $xp_y - yp_x$. Here, the particle 1 and 2 [Fig. 1(a)] are a photoelectron and a phtofragment, respectively, for the recoil frame photoelectron angular distribution (RFPAD). This AD function exhibits perfect rotational symmetry about the z axis but is antisymmetric when the coordinates are inverted on a plane including the z axis, while a single-particle AD with such symmetry does not exist.

This type of antisymmetry in AD will be attributed to the asymmetry of chiral molecules. As for RFPAD, a one-particle AD of particle 1 is asymmetric about the plane defined by the z axis and particle 2 [Fig. 1(b)], due to the left-right asymmetry of chiral molecules, including chiral isotopomers. For nonchiral molecules, including nonchiral isotopomers, the antisymmetric AD is strictly prohibited by symmetry principles [42,43]. The present Letter shows that chiral molecules having C_n, D_n, T, O, or I symmetry can be distinguished from nonchiral molecules on the basis of the reflection symmetry of the general vector correlation that occurs after irradiating gas phase molecules with unpolarized light. The symmetry of this vector correlation can be represented by a parity-odd second rank tensor. The emergence of this term will prove to be a rather universal phenomenon using the symmetry principles [44–48]. Following this, RFPAD is examined as an example of vector correlation [5,6,49,50] and numerical calculation results are shown for methyloxirane and a chiral isotopomer.

Seven limiting groups, known as the Curie groups [44–46], are required to express the symmetry of vector correlation and light polarization. Three of these,

$$K_h, D_{\infty h}, \text{ and } C_{\infty v}, \tag{1}$$

---

[*] Contact author: yoshiichisuzuki@hoku-iryo-u.ac.jp

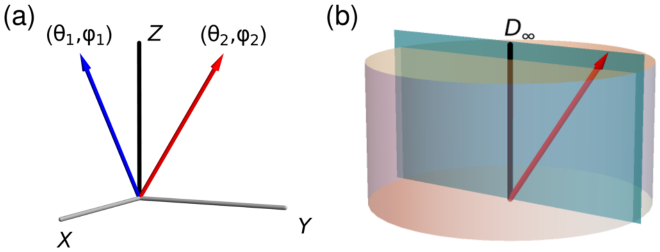

FIG. 1. (a) Geometrical arrangement of recoil-frame photoelectron angular distribution. Here the z axis is parallel to the photon k vector for the unpolarized light. The blue and red arrows correspond to the photoelectron (θ_1, φ_1) and recoil fragment (θ_2, φ_2), respectively. (b) Plane of symmetry defined by the D_∞ axis and a single particle (as indicated by the arrow) in $D_{\infty h}$ symmetry.

TABLE I. Characters of one-dimensional irreducible representations (Irrep) for selected elements of $D_{\infty h}$ and its subgroups. I, inversion; σ_h, reflection on the xy plane; σ_v, reflection on the plane that includes the ∞ axis. The twofold rotation is defined as $C_2' = \sigma_h\sigma_v$. The last column provides the spherical tensor $T_{LM}^{(\tau)}$ for rank L and component $M = 0$, where τ is an index indicating spatial inversion parity.

Irrep	E	I	σ_h	σ_v	C_2'	D_∞	C_∞	$C_{\infty h}$	$C_{\infty v}$	$T_{LM}^{(\tau)}$
Σ_g^+	1	1	1	1	1	Σ_1	Σ	Σ_g	Σ^+	$T_{00}^{(e)}, T_{20}^{(e)}$
Σ_u^+	1	−1	−1	1	−1	Σ_2	Σ	Σ_u	Σ^+	$T_{10}^{(o)}$
Σ_g^-	1	1	1	−1	−1	Σ_2	Σ	Σ_g	Σ^-	$T_{10}^{(e)}$
Σ_u^-	1	−1	−1	−1	1	Σ_1	Σ	Σ_u	Σ^-	$T_{00}^{(o)}, T_{20}^{(o)}$

are known as symmetries of atoms and linear molecules. Conversely, the remaining four,

$$K, D_\infty, C_\infty, \text{ and } C_{\infty h}, \tag{2}$$

do not appear as symmetries in single-particle three-dimensional distributions [51]. This is because a three-dimensional distribution function having an ∞ axis must possess a mirror plane that includes the ∞ axis. These four point groups appear in multiparticle distributions and in more general vector correlations. This is exactly the case for molecular chirality, which is defined by the relative positions of the atoms. The symmetry of such molecules, K, can be defined by rotational averaging while maintaining the relative positions of atoms, as occurs in the case of gas phase chiral molecules. Assuming that the symmetry of unpolarized light is $D_{\infty h}$ based on the electric dipole approximation, the symmetry of the system will equal the intersection

$$K \cap D_{\infty h} = D_\infty, \tag{3}$$

which lacks any rotoreflection symmetry. Even so, the symmetry of any single particle will be $D_{\infty h}$ based on a three-dimensional distribution. This is an example of Curie's symmetry principle [42], which states that "the effects produced can be more symmetrical than their causes" [43]. To make full use of this principle, it is necessary to consider the theory of irreducible tensors [9,30,52–57].

Constraints associated with the order of the tensor are included in the symmetry principle [46–48]. As an example, it is impossible to define a polar molecule using a specific symmetry operation such as spatial inversion. Instead, the symmetry of a polar molecule can be defined by a point group such that the parity-odd rank 1 tensor is totally symmetric. On this basis, methane (point group T_d) is not polar, even though the molecule lacks inversion symmetry [58].

The origin of this restriction on tensor order is perturbation theory. In the case of light-matter interactions, the electric dipole approximation is the lowest order. If we also use the rotating wave approximation, the interaction Hamiltonian can be expressed as $\hat{T} = \sqrt{4\pi/3}\sum_q \varepsilon_q^{\gamma *} r Y_{1,q}(\theta, \varphi)$. Here, ε_q^γ is a parity-odd first rank tensor and defines the polarization of light, γ is the index for purely polarized light, and any property of excited states, $|f\rangle = \sum_{i\neq 0} |i\rangle\langle i|\hat{T}|0\rangle$, can be expressed by a linear combination of tensor products $\varepsilon_{q'}\varepsilon_q^*$. These products are decomposed into the parity-even spherical tensor ρ_{LM}^γ of rank L and component M, $\rho_{LM}^\gamma = -\sum_{qq'}(-1)^{q'}\langle 1q1q'|LM\rangle \varepsilon_q^{\gamma *}\varepsilon_{-q'}^\gamma$ [59]. Due to the properties of the Clebsch-Gordan coefficients $\langle 1q1q'|LM\rangle$, L must be in the range $L = 0, 1, 2$.

Such tensor constraints are known as Yang's theorem [60] in scattering theory. According to this theorem and its extensions to account for odd L [1], light polarization [61], and vector correlations [31], the AD resulting from one-photon ionization with arbitrarily polarized light can be expanded using spherical tensors of rank 2 or less as

$$\frac{d\sigma}{d\Omega} = \sum_{L=0}^{2}\sum_{M}\rho_{LM}\sum_{\tau=o,e}U_{LM}^{(\tau)}(\Omega). \tag{4}$$

Here, Ω is a set of angular variables for a many-particle system, and $U_{LM}^{(\tau)}(\Omega)$ is a spherical tensor function. ρ_{LM} is the statistical tensor for the light, i.e., obtained by averaging ρ_{LM}^γ with weight w_γ ($\rho_{LM} = \sum_\gamma w_\gamma \rho_{LM}^\gamma$), and only ρ_{00} and ρ_{20} will have nonzero values in the case of unpolarized light [9,30,53–57]. To take into account vector correlations, an index τ is necessary to indicate the spatial inversion parity and is e or o for even or odd parity, respectively. It should also be noted that odd parity is possible only for chiral molecules [62] because ρ_{LM} is symmetrical under space inversion.

The function $U_{LM}^{(\tau)}(\Omega)$ obeys the same transformation law as the spherical tensor components $T_{LM}^{(\tau)}$. To determine the difference between D_∞ and $D_{\infty h}$, the axially symmetric components, $M = 0$, of the spherical tensor can be classified using the irreducible representations of $D_{\infty h}$ (Table I):

$$\Sigma_g^+ : U_{00}^{(e)}(\Omega),\ U_{20}^{(e)}(\Omega), \tag{5}$$

$$\Sigma_u^+ : U_{10}^{(o)}(\Omega), \tag{6}$$

$$\Sigma_g^- : U_{10}^{(e)}(\Omega), \text{ and} \tag{7}$$

$$\Sigma_u^- : U_{00}^{(o)}(\Omega),\ U_{20}^{(o)}(\Omega). \tag{8}$$

In Eq. (5), $U_{00}^{(e)}(\Omega)$ and $U_{20}^{(e)}(\Omega)$ are related to the integral cross section and the asymmetry parameter [63], respectively. Using circularly polarized light, the system symmetry can be C_∞ or $C_{\infty h}$ for chiral or nonchiral molecules, respectively. In addition, $U_{10}^{(o)}(\Omega)$ in Eq. (6) can appear as a single-particle AD of chiral molecules by circularly polarized light [1–3], while

$U_{10}^{(e)}(\Omega)$ in Eq. (7) has been observed in the case of spin polarization [64,65] and two-particle correlation [30–32,66,67] in conjunction with photoionization by circularly polarized light regardless of molecular chirality.

It is evident that the two components $U_{00}^{(o)}(\Omega)$ and $U_{20}^{(o)}(\Omega)$ in Σ_u^- will be totally symmetric in D_∞ [Eq. (8)]. As well, $U_{00}^{(o)}(\Omega)$ can be observed by Coulomb explosion imaging [36,37] although this requires the participation of at least three particles. For two-particle AD, the parity-odd second rank tensor $U_{20}^{(o)}(\Omega)$ is the sole chirality-sensitive component to be observed in one-photon processes with unpolarized light. An example of $U_{20}^{(o)}(\Omega)$ can be generated by an angular momentum addition. That is,

$$(x_1y_2 - x_2y_1)z_2 \propto \sin\theta_1 \sin\theta_2 \cos\theta_2 \sin(\varphi_1 - \varphi_2) \tag{9}$$

has the same symmetry as $U_{20}^{(o)}(\Omega)$.

For polynomial representations like Eq. (9), odd parity tensors $U_{LM}^{(o)}(\Omega)$ require at least degree 3, except for a vector $\boldsymbol{r} = (x, y, z)$, which is a parity-odd rank 1 tensor. The triple scalar product is an example of $U_{00}^{(o)}(\Omega)$, such as $(\boldsymbol{r}_1 \times \boldsymbol{r}_2) \cdot \boldsymbol{r}_3$ and $\boldsymbol{l}_1 \cdot \boldsymbol{r}_2$, where $\boldsymbol{l}_1$ is the angular momentum $\boldsymbol{r}_1 \times \boldsymbol{p}_1$. The latter suggests that angular momentum polarization is sensitive to molecular chirality, not only electron spin [17–19]. Another example is the one-particle AD function of xyz. This third rank tensor component describes the AD that occurs in the photoionization of a chiral molecule by two-photon linearly polarized light, predicted by Hansen and Berry [9] and discussed recently [10,62,68].

Until now, tensor components have often been obtained by controlling the polarization and subtracting or averaging the responses. For example, the difference

$$\frac{d\sigma^{\mathrm{LCP}}}{d\Omega} - \frac{d\sigma^{\mathrm{RCP}}}{d\Omega} = 2\rho_{10}\big[U_{10}^{(e)}(\Omega) + U_{10}^{(o)}(\Omega)\big]$$

can be obtained using left and right circularly polarized light, denoted by LCP and RCP, respectively. Recently, Fehre *et al.* observed molecular frame photoelectron angular distributions, which are three-particle ADs, using circularly polarized light and they obtained a circular dichroic response [40]. However, in a circular dichroic response, the parity-even $U_{10}^{(e)}(\Omega)$ is still left but parity-odd $U_{00}^{(o)}(\Omega)$ and $U_{20}^{(o)}(\Omega)$ are discarded. Alternatively, Tia *et al.* eliminated $U_{10}^{(e)}(\Omega)$ from $U_{10}^{(e)}(\Omega) + U_{10}^{(o)}(\Omega)$ via averaging over all azimuthal angles [33]. A potential issue of this averaging will be discussed later. Generally, the extraction of a lower symmetry response like $U_{10}^{(o)}(\Omega)$ will be accomplished using the projection operator.

It is possible to extract the chirality-dependent components $U_{L0}^{(o)}(\Omega)$ from the observed AD using symmetry operations. For a chiral molecule, the AD of its mirror image must be the same as the AD produced by inverting the laboratory coordinates, $\hat{I}d\sigma_R/d\Omega = d\sigma_S/d\Omega$, where an R/S index [69] distinguishes the R isomer of a chiral molecule from its mirror image (the S isomer) and $\hat{I}$ is the inversion operator for the laboratory coordinates of all particles represented by Ω. Therefore, the chirality-dependent component can be defined as

$$\mathrm{ChAD}(\Omega) = \frac{d\sigma_R}{d\Omega} - \frac{d\sigma_S}{d\Omega} \tag{10}$$

$$= (1-\hat{I})\frac{d\sigma_R}{d\Omega} \tag{11}$$

$$= 2\rho_{20}U_{20}^{(o)}(\Omega) \tag{12}$$

for two-particle ADs ($U_{00}^{(o)}(\Omega) = 0$) using linearly polarized or unpolarized light ($\rho_{10} = 0$). It should be noted that the reflection operators $\hat{\sigma}_h$ and $\hat{\sigma}_v$ can be used instead of $\hat{I}$. This is possible because, according to Table I, all improper rotations of $D_{\infty h}$ have the same effect on $U_{20}^{(o)}(\Omega)$. This property is attributed to the fact that D_∞ becomes $D_{\infty h}$ upon adding any one of three improper rotations. Hence, no matter which symmetry operation is used to antisymmetrize AD in Eq. (11), the same result should be obtained.

To further investigate the symmetry properties of $\mathrm{ChAD}(\Omega)$, this Letter explicitly focuses on the two-particle AD, $\mathrm{ChAD}(\theta_1, \theta_2, \varphi_{12})$, where θ_1 and θ_2 are the polar angles associated with particles 1 and 2 and φ_{12} is the difference in azimuthal angles, $\varphi_{12} = \varphi_1 - \varphi_2$. The symmetry properties

$$\mathrm{ChAD}(\pi-\theta_1, \pi-\theta_2, \varphi_{12}) = -\mathrm{ChAD}(\theta_1, \theta_2, \varphi_{12}) \tag{13}$$

and

$$\mathrm{ChAD}(\theta_1, \theta_2, -\varphi_{12}) = -\mathrm{ChAD}(\theta_1, \theta_2, \varphi_{12}) \tag{14}$$

can be derived using the reflection operators $\hat{\sigma}_h(\theta_i \to \pi - \theta_i)$ and $\hat{\sigma}_v(\varphi_i \to -\varphi_i)$. In addition, due to the D_∞ symmetry, $\mathrm{ChAD}(\theta_1, \theta_2, \varphi_{12})$ is symmetric with the twofold rotation C_2', leading to the transformation $\theta \to \pi - \theta$ and $\varphi \to -\varphi$. Interestingly, if the three angles $(\theta_1, \theta_2, \varphi_{12})$ are regarded simply as a point in Cartesian coordinates, C_2' can be interpreted as inversion about a point $(\frac{\pi}{2}, \frac{\pi}{2}, 0)$.

Equations (13) and (14) show that $\mathrm{ChAD}(\theta_1, \theta_2, \varphi_{12})$ has the nodal planes and nodal line

$$\varphi_{12} = 0, \pm\pi, \tag{15}$$

$$\theta_i = 0, \pi \quad (i = 1, 2) \text{ and} \tag{16}$$

$$\theta_1 = \theta_2 = \frac{\pi}{2}. \tag{17}$$

These equations can be regarded as degenerate based on the two vectors and one line along the ∞ axis in Fig. 1(a). That is, in the case of Eq. (15), the three elements are on the same plane whereas, for Eq. (16), one of the vectors overlaps the line and, for Eq. (17), both vectors are orthogonal to the line. In all cases, the figure has a plane of symmetry and therefore is nonchiral. In the theory of prochirality [38,70], this reflection symmetry has special importance, as explained below.

Certain considerations are associated with calculating $\mathrm{ChAD}(\theta_1, \theta_2, \varphi_{12})$ for *nonchiral* molecules. According to Mislow and Siegel [70], a nonchiral molecule can be made chiral by adding, removing, or substituting an atom at a point other than on the plane of symmetry. On the basis of this theorem, which we shall refer to as the chiralization theorem, nonchiral molecules may be mistakenly regarded as chiral molecules in the case that only one of the equivalent atoms or points exchanged by a symmetry operation is considered. During computational simulations, it is necessary to consider

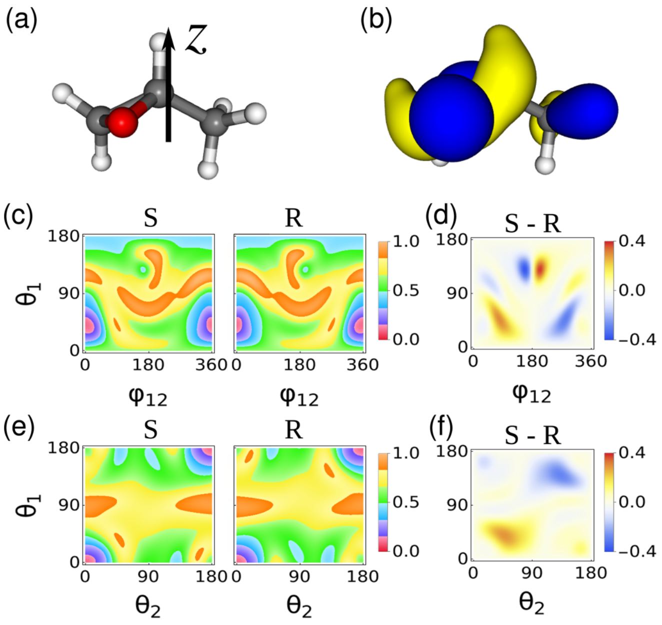

FIG. 2. (a) Molecular z axis of S-methyloxirane. (b) Second highest occupied molecular orbital. (c), (e) Photoelectron angular distributions of S- and R-methyloxirane for unpolarized light, assuming a photoelectron kinetic energy of 6.1 eV. In the case of (c), the angle (θ_2) between the molecular z axis and the laboratory z axis, which is parallel to the photon k vector, is assumed to be 45°. For (e) the relative azimuthal angle φ_{12} between the photoelectron and the molecular z axis is assumed to be 90°. (d), (f) Differences in photoelectron ADs between the S and R isomers based on (c) and (e).

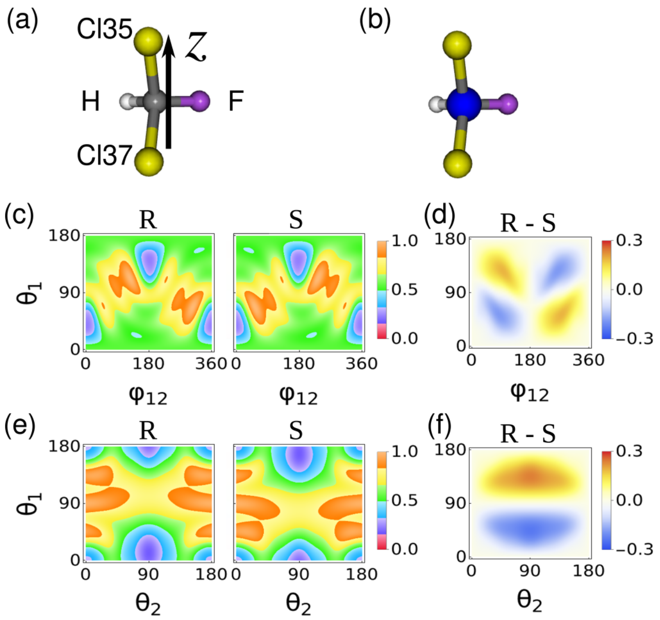

FIG. 3. (a) Molecular z axis of R-CHF^{35}Cl^{37}Cl. (b) Carbon 1s molecular orbital. (c), (e) Photoelectron angular distributions of R- and S-CHF^{35}Cl^{37}Cl for unpolarized light assuming a photoelectron kinetic energy of 2.1 eV. In the case of (c) the angle (θ_2) between the molecular z axis and the laboratory z axis, which is parallel to the photon k vector, is assumed to be 45°. For (e) the relative azimuthal angle φ_{12} between the photoelectron and the molecular z axis is assumed to be 90°. (d), (f) Differences in photoelectron ADs between the R and S isomers based on (c) and (e).

all such equivalent atoms simultaneously. In particular, it is important to note that nonchiral molecules having rotoreflection symmetry S_n do not possess a plane of symmetry, with the exception of point group $S_2(C_s)$. In calculations for such molecules, it is essential to average over equivalent atoms.

The above discussion concerning nonchiral molecules also has implications for *chiral* molecules. That is, a nonzero ChAD does not require chirality in the electronic wave functions for the initial and final (continuum) states. This relaxed condition is the same as that associated with Coulomb explosion imaging [36,37]. In fact, this Letter demonstrates that the ChAD of a chiral isotopomer will have the same order of magnitude as that of a typical chiral molecule even within the fixed nuclei approximation.

Prior to addressing the numerical calculations, it is helpful to examine the effect of light polarization on the chirality of ADs. The symmetry of two-particle AD can be D_∞ only for chiral molecules due to Eq. (3), when using unpolarized light. D_∞ symmetry has no rotoreflection symmetry, so it is chiral. This is also the case for linearly polarized light because the difference between unpolarized light and linearly polarized light is solely the value of ρ_{20}/ρ_{00}. Specifically, these values are $\sqrt{2}/2$ for unpolarized light and $-\sqrt{2}$ for linearly polarized light. Furthermore, by fixing the angles (θ_2, φ_2), the one-particle AD symmetries based on Eq. (4) as functions of θ_1 and φ_1 are chiral C_1 and nonchiral C_s for chiral and nonchiral molecules, respectively, due to the mirror plane in Fig. 1(b). Therefore, the microscopic molecular chirality is projected onto the chirality (D_∞ and C_1) of the macroscopic AD, not only for a two-particle AD but also for a single-particle AD.

In contrast, as reported by Pier *et al.* [38], in the case that circularly polarized light is employed, the ADs associated with coincident detection may be chiral even for a nonchiral molecule. The chiralization theorem is a useful means of examining this phenomenon. The symmetry of a nonchiral molecules in the gas phase will be K_h while the symmetry of circular polarization is $C_{\infty h}$. The resulting intersection will be nonchiral:

$$K_h \cap C_{\infty h} = C_{\infty h}. \tag{18}$$

According to the chiralization theorem, the symmetry of AD as a function of (θ_1, φ_1) has a chirality of C_1 or C_∞ depending on the fixed point (θ_2, φ_2) that is selected, assuming that this fixed point is not on the plane of symmetry in $C_{\infty h}$. In other words, the chirality observed using circular polarization is induced by the position of the detection device for the particle 2, rather than the chirality of the molecule [38].

In this Letter, RFPADs were calculated for methyloxirane and CHF^{35}Cl^{37}Cl, defining angles θ_1 and φ_1 based on the photoelectron k vector in the laboratory frame of Fig. 1(a). Because the dissociation processes of the molecular ions were unknown, uniaxially oriented molecules were incorporated into RFPADs [6,49,50]. The direction of particle 2 [Figs. 2(a) and 3(a)] was defined by the molecular z axis [71], meaning (θ_2, φ_2) in Fig. 1(a), and the rotational average of the molecule was taken around this axis. Although there is no atom that exactly represents particle 2, the hydrogen atom connected to the asymmetric carbon atom of methyloxirane and the ^{35}Cl atom of CFH ^{35}Cl ^{37}Cl are nearby the z axis.

Subsequently, the spherical tensors $U_{LM}^{(\tau)}(\theta_1, \theta_2, \varphi_{12})$ and Eq. (4) could be expanded as

$$\frac{d\sigma}{d\Omega} = \sum_{L_1 L_2 L} c_L^{(L_1 L_2)} \sum_M \rho_{LM} B_{LM}(L_1, L_2) \tag{19}$$

using bipolar harmonics [11,31,34,52]

$$B_{LM}(L_1, L_2) = \frac{4\pi}{[L_1][L_2]} \sum_{M_1 M_2} \langle L_1 M_1 L_2 M_2 | LM \rangle \times Y_{L_1 M_1}(\theta_1, \varphi_1) Y_{L_2 M_2}(\theta_2, \varphi_2) \tag{20}$$

where the coefficients $c_L^{(L_1 L_2)}$ are functions of bound-free transition dipole moments, $[x] = 2x + 1$, $\langle L_1 M_1 L_2 M_2 | LM \rangle$ are the Clebsch-Gordan coefficients, and τ in Eq. (4) is defined implicitly by the parity of $L_1 + L_2$, such as

$$U_{L0}^{(o)}(\theta_1, \theta_2, \varphi_{12}) = \sum_{L_1 + L_2 = \mathrm{odd}} c_L^{(L_1 L_2)} B_{L0}(L_1, L_2). \tag{21}$$

For example, Eq. (9) is proportional to $B_{2,0}(1, 2)$ with odd parity.

As for circular dichroic response ($L = 1$), the integration over azimuthal angles gives certainly the relationship $L_1 + L_2 = \mathrm{odd}$, due to the property of Clebsch-Gordan coefficients in Eq. (20). Although this averaging was used in the studies on RFPAD upon O(1s) photoionization [33,39], azimuth-dependent components were completely lost. The existence of azimuthal dependence of ChAD for circularly polarized light was demonstrated in Figs. S1–S3 of Supplemental Material [72] for O(1s) of methyloxirane. Specifically, with respect to $\varphi_{12} = 180^\circ$ in Fig. S2(d), the symmetric component is a chirality-sensitive component derived due to circularly polarized light, while there is only the asymmetric component in the case of unpolarized light [Fig. S1(d)]. Only the constant component remains in the azimuthal average (Fig. S3).

The coefficients $c_L^{(L_1 L_2)}$ are scalars because they do not depend on M. In contrast, these coefficients are affected by the rotation of the molecular coordinates. As an example, changing the direction of the z axis in Fig. 2(a) modifies the values of the coefficients. It is possible to show that these coefficients are tensors of rank L_2 with respect to the rotation of the molecular coordinates [72]. In addition, if a specific tensor contains the totally symmetric representation of the point group of the molecule, these coefficients will not become zero. For tensors that depend on the chirality of the molecule, the only condition is that $L_1 + L_2$ is an odd number, such that the rank L_2 is arbitrary. The symmetry of tensor coefficients $c_L^{(L_1 L_2)}$ in the molecular frame can be investigated using the effective operator formalism [73,74]. Such an analysis indicates that for all chiral point groups C_n, D_n, T, O, and I, $U_{20}^{(o)}(\theta_1, \theta_2, \varphi_{12})$ is nonzero [72]. Therefore, ChAD(Ω) is sensitive and specific to chirality because it is nonzero for all chiral molecules and only for chiral molecules.

It is noteworthy that nonchiral molecules may have nonzero coefficients $c_2^{(L_1, L_2)}$ with odd $(L_1 + L_2)$. One example is that $c_2^{(2,1)}$ of the C_s point group has a nonzero value [72]. Nevertheless, those coefficients must become zero after averaging over the equivalent atoms, as a particle 2, due to symmetry principles.

The bound-free transition dipole moments were calculated based on the equilibrium geometry as optimized using the second-order Møller-Plesset perturbation theory with the 6-31G* basis set. These calculations considered ionization from an initial orbital ϕ_0 to a continuum orbital with an effective single electron potential [75,76]. The initial orbitals ϕ_0 were obtained by Hartree-Fock/4-31G calculations. Continuum orbitals were obtained by the continuum multiple scattering Xα method and were then orthogonalized with all orbitals occupied [75,76]. The energy dependence of selected $c_L^{(L_1 L_2)}$ is shown in Fig. S4 of Supplemental Material [72].

Figures 2 and 3 present the RFPADs obtained for the molecular orbitals in Figs. 2(b) and 3(b). Here, the intensity has been normalized to the maximum value identified on a $20 \times 20 \times 20$ grid in the three-dimensional space of θ_1, θ_2, and φ_{12}. In Figs. 2(c) and 2(e), the difference between the RFPADs of the chiral molecule and its mirror image can be clearly seen. The difference values shown in Figs. 2(d) and 2(f) reach a magnitude of $\pm 35\%$ of the maximum value of AD for unpolarized light and $\pm 55\%$ for linearly polarized light, shown in Fig. S5 of Supplemental Material [72].

Figure 2(d) also clearly shows the angles at which ChAD($\theta_1, \theta_2, \varphi_{12}$) becomes zero as in Eqs. (15) and (16). In particular, Fig. 2(d) is antisymmetric with respect to the line $\varphi_{12} = 180^\circ$. Similarly, the center of Fig. 2(f) corresponds to the point at which ChAD becomes zero as expressed by Eq. (17), and Fig. 2(f) is antisymmetric with respect to the 180° rotation around this point.

Figure 3 demonstrates that the ChAD($\theta_1, \theta_2, \varphi_{12}$) of a chiral isotopomer CHF ^{35}Cl ^{37}Cl is of the same order of magnitude as that of an ordinary chiral molecule methyloxirane and that the ChAD does not require the electronic wave functions to be chiral. The latter means that in the calculations, electronic wave functions (bound and free) belonged to the a' or a'' symmetries of the C_s point group of CFHCl$_2$. Nonzero ChAD is due to the left-right asymmetry of the molecule [Fig. 3(a)], H on the left and F on the right, and the distinguishability of ^{35}Cl and ^{37}Cl. If both ^{35}Cl and ^{37}Cl are detected equally, another configuration H right and F left should be taken into account in the calculation, in which case the value of ChAD becomes zero.

In summary, the RFPAD is very sensitive to molecular chirality even without circular polarization. Moreover, due to the chiralization theorem, single-particle ADs are chiral only for chiral molecules when using linearly polarized and unpolarized light, as opposed to circularly polarized light. This phenomenon could potentially be used to perform time-resolved spectroscopy in conjunction with short pulses of linearly polarized light. This technique may also assist in explaining the origin of the homochirality of life based on light-matter interactions. To this end, it will be important to perform numerical calculations involving the dissociative photoionization of chiral molecules using realistic potential-energy surfaces.

This work was supported by JSPS KAKENHI Grant No. JP21H04970.

[1] B. Ritchie, Theory of the angular distribution of photoelectrons ejected from optically active molecules and molecular negative ions, Phys. Rev. A **13**, 1411 (1976).

[2] N. A. Cherepkov, Circular dichroism of molecules in the continuous absorption region, Chem. Phys. Lett. **87**, 344 (1982).

[3] N. Böwering, T. Lischke, B. Schmidtke, N. Müller, T. Khalil, and U. Heinzmann, Asymmetry in photoelectron emission from chiral molecules induced by circularly polarized light, Phys. Rev. Lett. **86**, 1187 (2001).

[4] S.-Y. Liu, K. Alnama, J. Matsumoto, K. Nishizawa, H. Kohguchi, Y.-P. Lee, and T. Suzuki, He I ultraviolet photoelectron spectroscopy of benzene and pyridine in supersonic molecular beams using photoelectron imaging, J. Phys. Chem. A **115**, 2953 (2011).

[5] A. V. Golovin, N. A. Cherepkov, and V. V. Kuznetsov, Photoionization of oriented molecules in a gas phase, Z. Phys. D **24**, 371 (1992).

[6] P. Downie and I. Powis, Molecule-frame photoelectron angular distributions from oriented CF_3I molecules, Phys. Rev. Lett. **82**, 2864 (1999).

[7] O. Kfir, P. Grychtol, E. Turgut, R. Knut, D. Zusin, D. Popmintchev, T. Popmintchev, H. Nembach, J. M. Shaw, A. Fleischer, H. Kapteyn, M. Murnane, and O. Cohen, Generation of bright phase-matched circularly-polarized extreme ultraviolet high harmonics, Nat. Photonics **9**, 99 (2015).

[8] T. Kaneyasu, Y. Hikosaka, M. Fujimoto, H. Iwayama, and M. Katoh, Controlling the orbital alignment in atoms using cross-circularly polarized extreme ultraviolet wave packets, Phys. Rev. Lett. **123**, 233401 (2019).

[9] J. C. Hansen and R. S. Berry, Angular distributions of electrons from resonant two-photon ionization of molecules, J. Chem. Phys. **80**, 4078 (1984).

[10] A. G. Harvey, Z. Mašín, and O. Smirnova, General theory of photoexcitation induced photoelectron circular dichroism, J. Chem. Phys. **149**, 064104 (2018).

[11] R. Uberna, R. D. Hinchliffe, and J. I. Cline, Photofragment μ-v-j correlation measured by $1+n'$ resonance-enhanced multiphoton ionization: Selective probing of bipolar moments and detection of chiral dynamics, J. Chem. Phys. **103**, 7934 (1995).

[12] A. Busalla, K. Blum, and D. G. Thompson, Collisions with chiral molecules prepared by optical pumping, J. Phys. B **33**, 2317 (2000).

[13] D. Patterson and J. M. Doyle, Sensitive chiral analysis via microwave three-wave mixing, Phys. Rev. Lett. **111**, 023008 (2013).

[14] A. Yachmenev and S. N. Yurchenko, Detecting chirality in molecules by linearly polarized laser fields, Phys. Rev. Lett. **117**, 033001 (2016).

[15] M. Nakamura, F. Palazzetti, P.-Y. Tsai, S.-J. Yang, K.-C. Lin, T. Kasai, D.-C. Che, A. Lombardi, and V. Aquilanti, Vectorial imaging of the photodissociation of 2-bromobutane oriented via hexapolar state selection, Phys. Chem. Chem. Phys. **21**, 14164 (2019).

[16] X. B. Planas, A. Ordóñez, M. Lewenstein, and A. S. Maxwell, Ultrafast imaging of molecular chirality with photoelectron vortices, Phys. Rev. Lett. **129**, 233201 (2022).

[17] N. Cherepkov, Polarization and orientation phenomena in photoionization of molecules, Adv. At. Mol. Opt. Phys. **34**, 207 (1994).

[18] N. A. Cherepkov and V. V. Kuznetsov, Photoionization of oriented molecules, Z. Phys. D **7**, 271 (1987).

[19] U. Heinzmann and N. A. Cherepkov, Spin polarization in photoionization, in *VUV and Soft X-Ray Photoionization*, edited by U. Becker and D. A. Shirley (Springer, New York, 1996), pp. 521–559.

[20] H. Kagan, A. Moradpour, J. F. Nicoud, G. Balavoine, and G. Tsoucaris, Photochemistry with circularly polarized light. Synthesis of optically active hexahelicene, J. Am. Chem. Soc. **93**, 2353 (1971).

[21] S. Mayer and J. Kessler, Experimental verification of electron optic dichroism, Phys. Rev. Lett. **74**, 4803 (1995).

[22] A. Owens, A. Yachmenev, S. N. Yurchenko, and J. Küpper, Climbing the rotational ladder to chirality, Phys. Rev. Lett. **121**, 193201 (2018).

[23] M. Leibscher, E. Pozzoli, A. Blech, M. Sigalotti, U. Boscain, and C. P. Koch, Quantum control of rovibrational dynamics and application to light-induced molecular chirality, Phys. Rev. A **109**, 012810 (2024).

[24] A. Buckingham, Chirality in NMR spectroscopy, Chem. Phys. Lett. **398**, 1 (2004).

[25] E. Hirota, Triple resonance for a three-level system of a chiral molecule, Proc. Jpn. Acad. Ser. **88**, 120 (2012).

[26] D. Patterson, M. Schnell, and J. M. Doyle, Enantiomer-specific detection of chiral molecules via microwave spectroscopy, Nature (London) **497**, 475 (2013).

[27] M. Leibscher, T. F. Giesen, and C. P. Koch, Principles of enantio-selective excitation in three-wave mixing spectroscopy of chiral molecules, J. Chem. Phys. **151**, 014302 (2019).

[28] V. Marichez, A. Tassoni, R. P. Cameron, S. M. Barnett, R. Eichhorn, C. Genet, and T. M. Hermans, Mechanical chiral resolution, Soft Matter **15**, 4593 (2019).

[29] A. F. Ordonez and O. Smirnova, Generalized perspective on chiral measurements without magnetic interactions, Phys. Rev. A **98**, 063428 (2018).

[30] R. L. Dubs, S. N. Dixit, and V. McKoy, Circular dichroism in photoelectron angular distributions from oriented linear molecules, Phys. Rev. Lett. **54**, 1249 (1985).

[31] J. Berakdar and H. Klar, Circular dichroism in double photoionization, Phys. Rev. Lett. **69**, 1175 (1992).

[32] T. Jahnke *et al.*, Circular dichroism in K-shell ionization from fixed-in-space CO and N_2 molecules, Phys. Rev. Lett. **88**, 073002 (2002).

[33] M. Tia *et al.*, Observation of enhanced chiral asymmetries in the inner-shell photoionization of uniaxially oriented methyloxirane enantiomers, J. Phys. Chem. Lett. **8**, 2780 (2017).

[34] R. N. Dixon, The determination of the vector correlation between photofragment rotational and translational motions from the analysis of Doppler-broadened spectral line profiles, J. Chem. Phys. **85**, 1866 (1986).

[35] J. Berakdar and H. Klar, Chiral multi-electron emission, Phys. Rep. **340**, 473 (2001).

[36] P. Herwig, K. Zawatzky, M. Grieser, O. Heber, B. Jordon-Thaden, C. Krantz, O. Novotný, R. Repnow, V. Schurig, D. Schwalm, Z. Vager, A. Wolf, O. Trapp, and H. Kreckel, Imaging the absolute configuration of a chiral epoxide in the gas phase, Science **342**, 1084 (2013).

[37] M. Pitzer, M. Kunitski, A. S. Johnson, T. Jahnke, H. Sann, F. Sturm, L. P. H. Schmidt, H. Schmidt-Böcking, R. Dörner, J. Stohner, J. Kiedrowski, M. Reggelin, S. Marquardt, A.

Schießer, R. Berger, and M. S. Schöffler, Direct determination of absolute molecular stereochemistry in gas phase by coulomb explosion imaging, Science **341**, 1096 (2013).

[38] A. Pier, K. Fehre, S. Grundmann, I. Vela-Perez, N. Strenger, M. Kircher, D. Tsitsonis, J. B. Williams, A. Senftleben, T. Baumert, M. S. Schöffler, P. V. Demekhin, F. Trinter, T. Jahnke, and R. Dörner, Chiral photoelectron angular distributions from ionization of achiral atomic and molecular species, Phys. Rev. Res. **2**, 033209 (2020).

[39] G. Nalin *et al.*, Photoelectron circular dichroism of O 1s-photoelectrons of uniaxially oriented trifluoromethyloxirane: energy dependence and sensitivity to molecular configuration, Phys. Chem. Chem. Phys. **23**, 17248 (2021).

[40] K. Fehre *et al.*, Fourfold differential photoelectron circular dichroism, Phys. Rev. Lett. **127**, 103201 (2021).

[41] Y.-I. Suzuki, Wave packet simulations for molecular orientation induced by circularly polarized light: Toward chiral resolution in the gas phase, Chem. Phys. Lett. **785**, 139134 (2021).

[42] L. D. Barron, *Molecular Light Scattering and Optical Activity*, 2nd ed. (Cambridge University, New York, 2009).

[43] M. Curie, *Pierre Curie* (Dover, New York, 1963).

[44] P. Curie, Sur la symétrie dans les phénomènes physiques, symétrie d'un champ électrique et d'un champ magnétique, J. Phys. Theor. Appl. **3**, 393 (1894).

[45] R. E. Newnham, *Properties of Materials: Anisotropy, Symmetry, Structure* (Oxford University, New York, 2005).

[46] S. T. Lagerwall, *Ferroelectric and Antiferroelectric Liquid Crystals* (Wiley, New York, 1999).

[47] R. R. Birss, *Symmetry and Magnetism*, 2nd ed. (North-Holland, Amsterdam, 1966).

[48] A. S. Nowick, *Crystal Properties via Group Theory* (Cambridge University, New York, 1995).

[49] R. R. Lucchese, A simple model for molecular frame photoelectron angular distributions, J. Electron Spectrosc. **141**, 201 (2004).

[50] D. Dowek, M. Lebech, J. C. Houver, and R. R. Lucchese, Circular dichroism in molecular frame photoemission, Mol. Phys. **105**, 1757 (2007).

[51] K. Mislow, Molecular chirality, in *Topics in Stereochemistry* (Wiley, New York, 1999), pp. 1–82.

[52] D. M. Brink and G. R. Satchler, *Angular Momentum*, 2nd ed., Oxford Library of the Physical Sciences (Clarendon, Oxford, 1968).

[53] V. L. Jacobs, Theory of atomic photoionization measurements, J. Phys. B **5**, 2257 (1972).

[54] K. Bonhoff, S. Nahrup, B. Lohmann, and K. Blum, Angular distribution of molecular Auger electrons, J. Chem. Phys. **104**, 7921 (1996).

[55] S. Motoki, J. Adachi, K. Ito, K. Ishii, K. Soejima, A. Yagishita, S. K. Semenov, and N. A. Cherepkov, Complete photoionization experiment in the region of the $2\sigma_g \rightarrow \sigma_u$ shape resonance of the N_2 molecule, J. Phys. B **35**, 3801 (2002).

[56] A. N. Grum-Grzhimailo, On the angular distributions in molecular photoionization beyond the dipole approximation, J. Phys. B **36**, 2385 (2003).

[57] Y.-I. Suzuki and T. Suzuki, Determination of ionization dynamical parameters by time-resolved photoelectron imaging, Mol. Phys. **105**, 1675 (2007).

[58] Similarly, it is possible to define a chiral molecule by a point group such that the pseudoscalar, the parity-odd rank zero tensor, is totally symmetric.

[59] This is an addition of two contragredient tensors [52] ε_q^* and $(-1)^{q'}\varepsilon_{-q'}$, resulting in a contragredient tensor ρ_{LM}. Here, a contragredient tensor S_{lm} can be defined by a complex conjugate of a tensor T_{lm}, a cogredient tensor, where $S_{lm} = T_{lm}^*$. They obey the transformation rules for the rotation defined by the Euler angles $\hat{R} = (\alpha, \beta, \gamma)$, $T'_{ls} = \sum_q T_{lq} D^l_{qs}(\hat{R})$, and $S'_{ls} = \sum_q S_{lq} D^{l*}_{qs}(\hat{R}) = (-1)^{q-s} \sum_q S_{lq} D^l_{-q,-s}(\hat{R})$, using rotation matrices. The last equation indicates that $(-1)^q S_{l,-q}$ is a cogredient tensor of rank l and component q, and hence $(-1)^{q'}\varepsilon_{-q'}$ is a contragredient tensor of rank 1 and component q'. In addition, a minus sign is added for $\sum_{qq'}$ to make ρ_{00} positive.

[60] C. N. Yang, On the angular distribution in nuclear reactions and coincidence measurements, Phys. Rev. **74**, 764 (1948).

[61] U. Fano and D. Dill, Angular momentum transfer in the theory of angular distributions, Phys. Rev. A **6**, 185 (1972).

[62] Y.-I. Suzuki, Improved chiral photoelectron spectroscopy via selection of chirality-selective molecular axis orientations: A theoretical analysis of non-negative smooth functions, Phys. Rev. Lett. **130**, 143202 (2023).

[63] J. Cooper and R. N. Zare, Angular distribution of photoelectrons, J. Chem. Phys. **48**, 942 (1968).

[64] U. Fano, Spin orientation of photoelectrons ejected by circularly polarized light, Phys. Rev. **178**, 131 (1969).

[65] J. Kessler and J. Lorenz, Experimental verification of the Fano effect, Phys. Rev. Lett. **24**, 87 (1970).

[66] K. Soejima, A. Danjo, K. Okuno, and A. Yagishita, Linear and circular dichroism in the double photoionization of helium, Phys. Rev. Lett. **83**, 1546 (1999).

[67] O. Geßner, Y. Hikosaka, B. Zimmermann, A. Hempelmann, R. R. Lucchese, J. H. D. Eland, P.-M. Guyon, and U. Becker, $4\sigma^{-1}$ inner valence photoionization dynamics of NO derived from photoelectron-photoion angular correlations, Phys. Rev. Lett. **88**, 193002 (2002).

[68] A. F. Ordonez and O. Smirnova, Disentangling enantiosensitivity from dichroism using bichromatic fields, Phys. Chem. Chem. Phys. **24**, 7264 (2022).

[69] R. S. Cahn, C. Ingold, and V. Prelog, Specification of molecular chirality, Angew. Chem., Int. Ed. Engl. **5**, 385 (1966).

[70] K. Mislow and J. Siegel, Stereoisomerism and local chirality, J. Am. Chem. Soc. **106**, 3319 (1984).

[71] These z axes are defined by c and a axes of inertia for methyloxirane and $CFHCl_2$ (a nonchiral isotopomer), respectively.

[72] See Supplemental Material at http://link.aps.org/supplemental/10.1103/PhysRevA.109.L060802 for details of the symmetry of $c_L^{(L_1 L_2)}$, implications for photoelectron spin, additional figures for methyloxirane, which includes Refs. [77–85].

[73] L. Barron, Optical activity and time reversal, Mol. Phys. **43**, 1395 (1981).

[74] Y.-I. Suzuki, Communication: Photoionization of degenerate orbitals for randomly oriented molecules: The effect of time-reversal symmetry on recoil-ion momentum angular distributions, J. Chem. Phys. **148**, 151101 (2018).

[75] D. Dill and J. L. Dehmer, Electron-molecule scattering and molecular photoionization using the multiple-scattering method, J. Chem. Phys. **61**, 692 (1974).

[76] Y.-I. Suzuki and T. Suzuki, Photoelectron angular distribution in valence shell ionization of heteroaromatic molecules studied by the continuum multiple scattering Xα method, J. Phys. Chem. A **112**, 402 (2008).

[77] R. N. Zare, *Angular Momentum: Understanding Spatial Aspects in Chemistry and Physics* (Wiley, New York, 1988).

[78] D. Dill, Fixed-molecule photoelectron angular distributions, J. Chem. Phys. **65**, 1130 (1976).

[79] N. A. Cherepkov and G. Raseev, Photoionization of oriented CO molecule: Linear dichroism in the angular-distribution of photoelectrons, J. Chem. Phys. **103**, 8238 (1995).

[80] Y. Suzuki and T. Seideman, Mapping rotational coherences onto time-resolved photoelectron imaging observables, J. Chem. Phys. **122**, 234302 (2005).

[81] P. Hockett and V. Makhija, Topical review: Extracting molecular frame photoionization dynamics from experimental data, J. Phys. B **56**, 112001 (2023).

[82] Y.-I. Suzuki, Circular dichroism in photoionization of degenerate orbitals: Spin-polarized photoelectrons and spontaneous separation of oriented photoions, J. Chem. Phys. **149**, 204312 (2018).

[83] A. Gelessus, W. Thiel, and W. Weber, Multipoles and symmetry, J. Chem. Edu. **72**, 505 (1995).

[84] Y.-I. Suzuki, Direct relation of molecular orbital symmetry with photoelectron angular distributions from aligned molecules in the gas phase, J. Phys. B **41**, 215204 (2008).

[85] N. A. Cherepkov, Manifestations of the optical activity of molecules in the dipole photoeffect, J. Phys. B **16**, 1543 (1983).